Optimized Multistandard RF Subsampling Receiver Architecture

Rim Barrak, Adel Ghazel, *Senior Member, IEEE*, and Fadhel Ghannouchi, *Fellow, IEEE*

***Abstract*—This paper presents a novel subsampling-based down-conversion topology for multistandard radio receiver design. This receiver topology is based on two subsampling stages. The first stage has a fixed RF subsampling frequency; however, the IF sampling frequency of the second stage is variable and depends on the standard being considered. This approach overcomes various undesirable effects related to the sampling frequencies and noise aliasing. By optimizing the choice of the RF subsampling clock frequency, complete multistandard RF bands are down-converted to the same IF band. Quadrature baseband channel downconversion is achieved by a tunable IF sampling frequencies clock. A tunable band-pass RF filter and an IF band-pass filter are designed to perform anti-aliasing and limit wideband noise. A generic design methodology is proposed and validated through its application to a GSM, UMTS and IEEE-802.11g multistandard receiver. Simulation results of this receiver design example confirm the validation of proposed subsampling receiver topology and show the efficiency of the design methodology.**

***Index Terms*—Anti-aliasing, multistandard receiver, radio receiver, RF subsampling, sampling noise.**

I. Introduction

FOR the last two decades, commercial success of wireless digital communication systems has enabled the continual development of radio communication standards, introducing new mobile services from high-quality voice to high bit rate data and multimedia communications [1-4]. Important academic and industrial research has been carried out, leading to the design and manufacturing of low-power wireless equipment with high integration for each radio communication standard. Today, the new commercial challenge in the enhancement of mobile technology is the development of multistandard software defined radio (SDR) based wireless mobile equipment that offer end-users multimode and multi-service facilities with the use of low-cost, low-power and highly integrated devices.

The ultimate approach in achieving multimode operation is to design multistandard radio receiver hardware that can be reconfigured by software, with maximum hardware functionality sharing between the various standards. High selective narrow-band superheterodyne radio frequency (RF) architectures, however, are difficult to realize in practice; and, since they are not considered as valuable solutions for new wideband or multistandard applications, three main wideband receiver architectures were recently developed for these applications [5]. The first one, wideband intermediate frequency (IF) architecture (WB-IF), converts the entire RF band to IF using a fixed local oscillator (LO) frequency and high-performance balanced down-converter, such as the six-mixer configuration based on the Weaver technique, in order to ensure high image rejection performance. It has the disadvantage of using a large number of analog components, which increases power consumption and reduces receiver integrability and flexibility.

The second one, IF sampling architecture, down-converts RF channels to a fixed IF using a tunable LO and then performs a second frequency down-conversion using a band-pass analog-to-digital conversion (ADC). This architecture imposes a more stringent dynamic range for the ADC stage due to IF sampling. The third one, direct conversion architecture, down-converts RF signals directly to baseband, increasing receiver integrability and flexibility. However, this analog architecture suffers from a DC offset problem and requires highly accurate phase and gain matching between quadrature LOs and signal paths, which imposes large constraints on LO specifications in terms of tunable range and phase noise.

To overcome analog down-conversion constraints, a new design approach based on a radio frequency (RF) subsampling technique has recently been proposed so that integrable RF receiver front-end architectures for Global System for Mobile communication (GSM) [6], wireless local area network (WLAN) [7] and Bluetooth [8] can be designed. These architectures are based on switched-capacitor (SC) circuits to perform discrete-time processing after sampling. This leads to excellent improvement in radio receiver performance, integration and low-power dissipation, but the designed RF front-end receivers are optimized for only a single standard [6-8]. Multistandard operation and adaptability need a tunable sampling frequency for each RF band and for each carrier frequency in the same band. This implies difficult constraints on sampling clock specifications, in terms of tunable range and phase noise. A low sampling frequency is required to reduce power consumption of the ADC; however, it increases track-and-hold (T&H) circuit aperture jitter noise and subsampled thermal noise. All of these constraints provided the motivation for the subject of this paper, in that definitions of appropriate design solutions are needed to take advantage of this new RF architectural concept.

In this paper, a novel RF subsampling-based down-

Manuscript received June 1, 2007; revised September 12, 2007; accepted July 3, 2008. The associate editor coordinating the review of this paper and approving it for publication was K. Sowerby.

R. Barrak and A. Ghazel are with Cirta'Com Laboratory, Ecole Supérieure des Communications de Tunis, 2088 Cité technologique des Communications El Ghazala - Ariana - Tunisia (e-mail: {rim.barrak, adel.ghazel}@supcom.rnu.tn).

F. Ghannouchi is with Intelligent RF Radio Laboratory, Electrical and Computer Engineering Department, University of Calgary, Calgary, Alberta, Canada T2N 1N4 (e-mail: fghannouchi@ucalgary.ca).

Digital Object Identifier 10.1109/TWC.2009.070584

1536-1276/09$25.00 © 2009 IEEE

Authorized licensed use limited to: Suzanne Habib. Downloaded on February 20,2025 at 15:04:44 UTC from IEEE Xplore. Restrictions apply.

Exhibit 1020
Nokia of America Corporation, et al. v. Smart RF Inc.
Page 000001

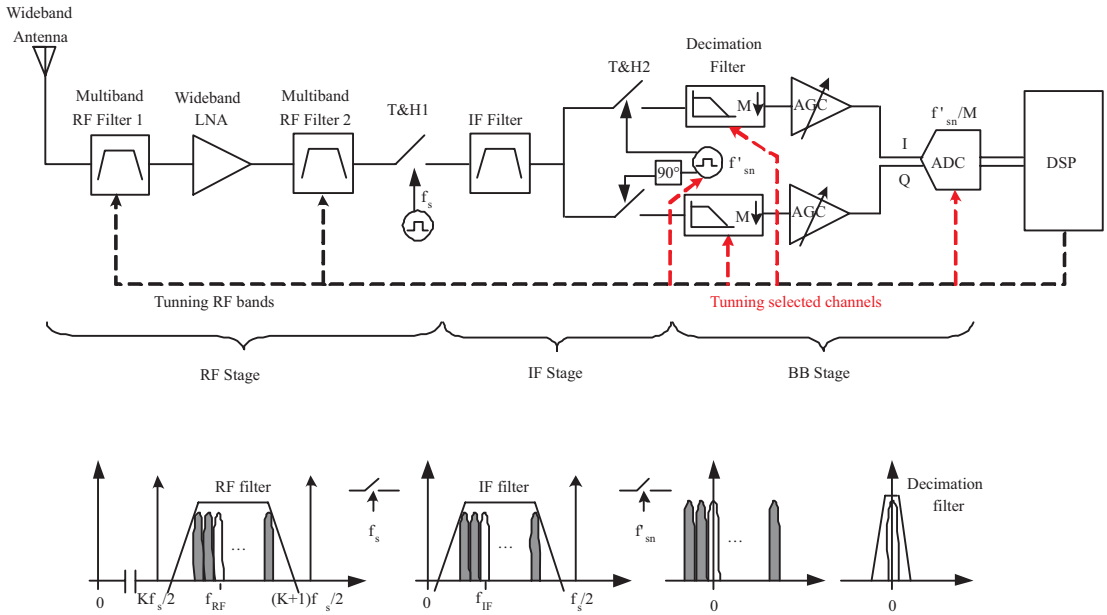

Fig. 1. Multistandard RF subsampling receiver architecture.

conversion receiver topology is proposed to enhance programmability and integrability of the multistandard radio receiver. The proposed contributions presented in this paper concern radio system topology adapted to the subsampling processing of multistandard signals with new design solutions that overcome noise and aliasing constraints. An efficient and generic design methodology is established analytically for the receiver circuit's specifications. To validate the proposed receiver RF subsampling topology and design methodology, a multistandard GSM, Universal Mobile Telecommunications System (UMTS) and IEEE-802.11g radio is considered as the application example on which the SDR multistandard design and system performance analyses were carried out.

The paper is organized as follows. Section II highlights design advantages of the new proposed RF subsampling architecture that enables multistandard signal processing. Receiver stage design considerations are established in section III, in terms of subsampling frequencies selection, subsampling circuits, and RF and IF filter specifications. The defined design methodology is considered in section IV to optimize the subsampling frequency plan and circuits design for a GSM, UMTS and IEEE-802.11g multistandard radio receiver. System level simulation results, using Advanced Design System (ADS) simulator from Agilent Technologies [9], are presented in section V for the design performance analyses.

II. Multistandard RF Subsampling Receiver Definition

Radio receiver design based on the RF subsampling concept offers excellent improvement in terms of integration and power dissipation reduction, compared to analog down-conversion techniques. For multistandard applications, the processing of multiband and multi-carrier signals with conventional receiver structures puts more constraints on filter design and increases sampling noise effects. To overcome these limitations and take advantage of the RF subsampling concept, a new multistandard RF subsampling radio receiver topology is defined, as described herein, to efficiently handle multiband signals aliasing issues and to reduce T&H noise effects.

Downstream from the antenna, a tunable band-pass RF filter is first used to perform the complete RF band selection and contribute to image frequency rejection for each received radio standard signal. The low noise amplifier (LNA) needs to achieve wideband high gain and low noise for each standard. To allow for the use of conventional wideband LNA, it is proposed that a second RF filter, which will attenuate wideband noise amplified by the LNA and provide enough protection against the noise aliasing generated by the subsampling operation, be added in the receiver path after the LNA.

The subsampling-based down-conversion stage topology design depends on the sampling frequency choice. The most important design constraints for the sampling frequency choice are related to T&H aperture jitter noise and subsampled thermal noise. These noises can be limited by increasing sampling frequency, but a value that is too high is not suitable for the ADC, since it will generate excessive power dissipation. To reach the best compromise for the sampling frequency choice, while complying with the stringent constraints on both the T&H and ADC circuits, we propose to operate the subsampling in two stages. Hence, the first subsampling stage, using a relatively high fixed RF sampling frequency (f_s), will be designed to translate all RF bands with in-band blockers and interferers to the same IF band located in *[0 f_s/2]*. A second subsampling stage, using a variable IF sampling frequency (f'_{sn}), will be designed to reduce the sampling rate and allow for the desired channel down-conversion to baseband. Complex (inphase, quadrature) down-conversion from IF to baseband is proposed to separate the desired band from its image.

Adjustable sampling rate conversion from f_s to f'_{sn} can be achieved either by an interpolation-decimation operation

Authorized licensed use limited to: Suzanne Habib. Downloaded on February 20,2025 at 15:04:44 UTC from IEEE Xplore. Restrictions apply.

Exhibit 1020
Nokia of America Corporation, et al. v. Smart RF Inc.
Page 000002

or by analog filtering and resampling, in order to sufficiently attenuate channel images that can alias into the baseband. The first method can be achieved using discrete-time processing, but it requires complex calculations due to the fact that f_s is constant and f'_{sn} depends on the multistandard IF channel position. Hence, we choose to use the second solution, analog filtering and resampling.

To further reduce the dynamic range and sampling rate at the ADC input, the second subsampling stage is followed by a discrete-time low-pass decimation filter and then an automatic gain control (AGC).

According to these design considerations for multistandard RF signal processing, the new RF subsampling receiver structure, as represented in Fig. 1, is defined by the authors to obtain significant design advantages at the RF system level, compared to other proposed RF sampling architectures [6-8].

III. RF Subsampling Receiver Design Principle

Through the multistandard RF subsampling topology, all RF channels are down-converted to baseband without aliasing, as long as the Nyquist criterion is fulfilled for each channel bandwidth. The main drawbacks of this topology are the wideband noise folding into the baseband and T&H circuit noise sources. An efficient and generic design methodology is presented in this section for multistandard receiver circuit specifications.

A. First subsampling frequency optimization

The first subsampling frequency, generated by the sampling rate f_s of the T&H circuit, needs to be defined to allow for the down-conversion to IF of multistandard RF signals with multiple carrier frequency values and different RF bands. In order to ensure aliasing of the RF signals bandwidth and avoid overlap of the aliased bands, the resulting intermediate band center frequency, f_{IF}, in *[0 f_s/2]* region, for a given f_s, can be calculated by (1) depending on *K*, parity [10-11]. If *K* is even, we then obtain the original signal atf_{IF}; or, we obtain the mirrored signal.

$$if\ K = \left(\frac{f_c}{\frac{f_s}{2}}\right)\begin{cases} is\ even,\ f_{IF} = rem(f_c, f_s) \\ is\ odd,\ f_{IF} = f_s - rem(f_c, f_s) \end{cases} \quad (1)$$

where, f_c is the whole RF band center frequency, *fix(a)* is the truncated integer portion of argument *a*, and *rem(a,b)* is the remainder after the division of *a* by *b*. f_{IF} has to verify conditions (2) and (3) in order to avoid overlap [11].

$$f_s/2 > f_{IF} - B/2 \quad (2)$$

$$f_{IF} > B/2 \quad (3)$$

where, *B* is the whole RF bandwidth.

In multimode operation, diverse RF bands have to be processed consecutively in the multistandard receiver. For each RF band, the down-converted position, f_{IF}, is calculated by (1), while respecting the constraints of conditions (2) and (3). In the case of *N* standards, all RF bands are translated after RF subsampling to the same IF band defined by $\bigcup_{i=1}^{N} BT_i$, where BT_i corresponds to the translated IF sub-band with respect to the standard, *i*. The IF band is composed of the *N* IF sub-bands

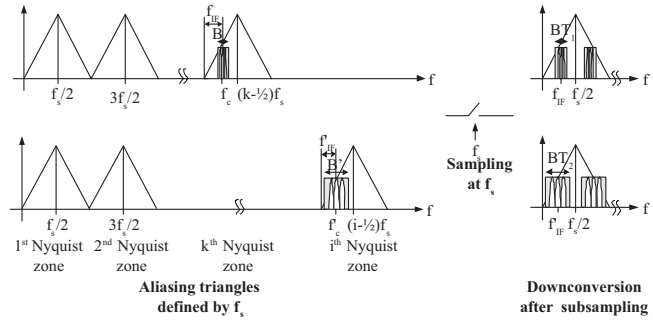

Fig. 2. Frequency down-conversion for dual-standard selectable subsampling receiver.

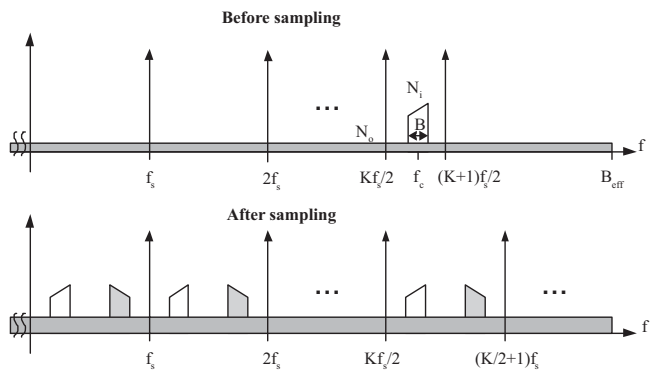

Fig. 3. Noise folding effect as a result of subsampling.

that can be close to one another. Fig. 2 shows a graphical representation of the dual-standard frequency down-conversion example. Out-of-band noise is aliased and combined into each *f_s/2* band, due to signal spectrum periodicity created by the subsampling operation. The signal to noise ratio, SNR_{out}, at the T&H output, due to noise folding by subsampling can be approximated by (4) [10].

$$SNR_{out} = \frac{P_S}{N_i + (n-1)N_o},\ where\ n = fix\left(\frac{2B_{eff}}{f_s}\right) \quad (4)$$

where, *n* represents the noise folding effect; P_S is the band-pass signal power; N_i and N_o are the in-band and the out-of band noise power spectral densities before sampling, respectively; and, B_{eff} is the effective noise bandwidth. The noise folding effect is illustrated in Fig. 3. SNR_{out} can be kept relatively unaffected by Track-and-Hold thermal noise, by providing enough RF front-end gain. In most communication systems, the out-of-band noise (interferers, blockers) has similar, even higher levels than the in-band noise. To avoid signal to noise degradation due to subsampling, we propose the use of an anti-aliasing band-pass RF filter before the first T&H circuit, as shown in Fig. 1, to sufficiently attenuate the out-of-band noise [12]. The first images to be rejected before subsampling operation are centered at $2f_{IF}$ and f_s-$2f_{IF}$. For symmetrical anti-aliasing filter design, images have to be evenly spaced. This corresponds to f_{IF} = *f_s/4*. In the case of multistandard signals, we added condition (5) as a novel constraint for the f_s choice, in order to alleviate second RF filter design and bring different RF bands to the same IF

Authorized licensed use limited to: Suzanne Habib. Downloaded on February 20,2025 at 15:04:44 UTC from IEEE Xplore. Restrictions apply.

Exhibit 1020
Nokia of America Corporation, et al. v. Smart RF Inc.
Page 000003

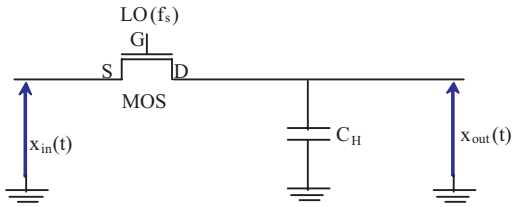

Fig. 4. Track-and-hold circuit.

band, around $f_s/4$. This minimizes the distance between the IF band center frequency relative to signals of radio standard i (f_{IFi}) and $f_s/4$.

$$min\Big(\sum_{i=1}^{N}\Big|f_{IFi}-\frac{f_s}{4}\Big|^2\Big) \tag{5}$$

B. Second subsampling frequencies determination

The second subsampling frequency f'_{sn}, with respect to channel number n, should be equal to the desired channel center frequency at IF band (f_{IFn}) or its sub multiple frequency. Also, in order to avoid channel aliasing, f_{IFn} should be higher than channel bandwidth (B_{chn}). Then, f'_{sn} should be selected from expression (6).

$$f'_{sn}=\frac{f_{IFn}}{m}, m=1,2,...,fix\Big(\frac{f_{IFn}}{B_{chn}}\Big) \tag{6}$$

The images of bandwidth (B_{chn}) are centered at f_{images} around f_{IFn}. f_{images} are given by (7).

$$f_{images}=f_{IFn}\pm kf'_{sn}, k=1,2,... \tag{7}$$

The second subsampling frequency f'_{sn} is chosen as equal to its highest value corresponding to f_{IFn} in order to relax the IF filter specifications. The first image frequencies are then located at $B_{ch}/2$ and $2.min(f_{IFn})-B_{ch}/2$, where $min(f_{IFn})$ is the lowest intermediate frequency.

By choosing a fixed frequency for the first subsampling stage, all multistandard RF bands are translated to the same IF band. This gives the advantage of using one band-pass IF filter, which is designed to satisfy multistandard anti-aliasing specifications for all channels. The design of a single IF filter adds another constraint, formulated by expression (8), for the choice of f_s.

$$max(f_{IFn}+B_{chn}/2)<min(2f_{IFn}-B_{chn}/2) \tag{8}$$

C. Track-and-hold circuit specifications

A T&H circuit, as shown in Fig. 4, is composed of an NMOS transistor, with internal resistance R_{on}, as a sampling switch and a holding capacitor, C_H. For an RF sampling operation, there is a number of nonidealities that limit the T&H circuit performance, such as finite acquisition time, sampling pedestal, thermal noise and aperture jitter noise [13]. In this section, we propose to determine the design specifications of the T&H circuit by considering the T&H speed-accuracy-thermal noise trade-off and the aperture jitter noise generated essentially from sampling clock phase noise. The sampling frequency, f_s, has to be chosen to efficiently handle multiband signal aliasing issues and to properly reduce T&H noise effects.

For T&H speed evaluation, the analog input bandwidth is considered. If we assume that, in the track mode, the T&H circuit is equivalent to a first-order low-pass filter, then the analogue bandwidth (B_{ana}) defined at 3 dB attenuation can be equivalent to $1/(2\pi T_{on})$, where T_{on} denotes the acquisition time. It is expressed as:

$$T_{on}=R_{on}C_H \tag{9}$$

To improve T&H circuit speed, C_H has to be reduced.

For T&H accuracy evaluation, the sampling pedestal error is considered. This error is related to the NMOS transistor channel charge injection into C_H during the transition from track mode to hold mode. It can be expressed as [14]:

$$\Delta V_C=-\frac{C_{ox}WL}{2C_H}(V_{GS}-V_T) \tag{10}$$

where, C_{ox} is the gate oxide capacitance; W and L are the transistor width and length, respectively; V_{GS} is the gate source voltage; and, V_T is the threshold voltage. A dummy switch compensation technique can be implemented with the basic T&H circuit, in order to improve accuracy [15]. Also, in practice, the T&H circuit would be differential to reduce even-order nonlinear distortions.

The T&H thermal noise is generated from the transistor resistance, R_{on}, which is controlled by C_H. It will be subsampled and aliased into each Nyquist band, which leads to high SNR degradation. This effect cannot be avoided by the anti-aliasing filter placed before the T&H circuit. Assuming a duty cycle, β, of 0.5, which corresponds to a track time equal to hold time, the thermal noise power generated in the signal channel band, B_{ch}, at the T&H circuit output is given by (11) [16].

$$P_{Nt}|_{dBw}=10log\Big(\beta^2\frac{2kTB_{ch}}{f_sC_H}\Big) \tag{11}$$

where, k is Boltzmann's constant, and T is the absolute temperature. In order to neglect the effects of the subsampled noise, the latter must be less than the receiver noise floor expressed at the T&H input, which is given by (12).

$$P_{N_floor}|_{dBm}=P_{sens}|_{dBm}+G|_{dB}-SNR_{min}|_{dB} \tag{12}$$

where, P_{sens} is the receiver sensitivity, G is receiver front-end gain, and SNR_{min} is the minimum signal to noise ratio at the demodulator input to meet the bit error rate (BER) requirements.

To improve T&H accuracy and reduce T&H subsampled thermal noise, C_H has to be increased. Hence, the T&H speed-accuracy-thermal noise trade-off can be realized by considering the C_H design parameter.

The T&H aperture jitter gives rise to an induced noise, due to the mixing of the desired signal with high level blocking signals. By assuming that Δt is the total aperture jitter, the signal to noise ratio due to jitter, SNR_j, is given by (13) [17].

$$SNR_j=-20log(2\pi f_c\Delta t) \tag{13}$$

However, SNR_j is limited to maximum blocker level attenuation A_{tt} given by expression (14), combined with an over

Authorized licensed use limited to: Suzanne Habib. Downloaded on February 20,2025 at 15:04:44 UTC from IEEE Xplore. Restrictions apply.

Exhibit 1020
Nokia of America Corporation, et al. v. Smart RF Inc.
Page 000004

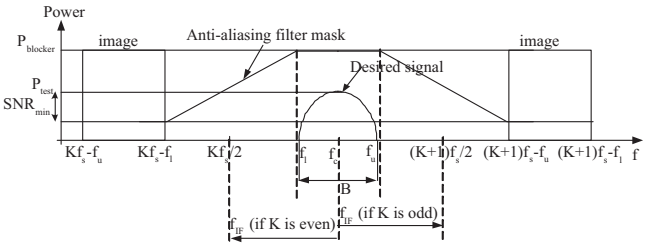

Fig. 5. Anti-aliasing band-pass filter specifications.

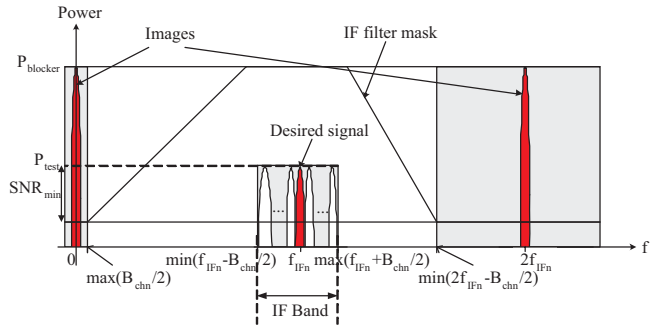

Fig. 6. IF filter specifications.

sampling gain, G_{os}, given by (15).

$$A_{tt}|_{dB} = P_{blocker}|_{dBm} - (P_{test}|_{dBm} - SNR_{min}|_{dB}) \quad (14)$$

$$G_{os} = 10log\left(\frac{f_s}{2B_{ch}}\right) \quad (15)$$

where, $P_{blocker}$ is maximum blocker power, and P_{test} is the desired test signal power.

The maximum allowed aperture jitter can be transformed to a sampling clock phase noise, evaluated at the maximum blocker level using expression (16) [18].

$$PN|_{dBc/Hz} = -A_{tt}|_{dB} - 20log\left(\frac{f_c}{f_s}\right) - 10log(B_{ch}) \quad (16)$$

The maximum input signal to T&H circuit is equal to the maximum receiver input signal, P_{max}, amplified by G. Then, the dynamic range at T&H is given by (17).

$$DR|_{dB} = P_{max}|_{dBm} + G - P_{N_floor}|_{dBm} \quad (17)$$

D. Filter specifications

The proposed multistandard RF subsampling radio receiver structure, as illustrated in Fig. 1, uses two RF filters and an IF filter. The first RF filter is a band-pass filter that is designed to attenuate the out-of-band blockers and bring them to the same level as in-band blockers. The second RF filter is also a band-pass filter, but is designed to select the whole RF band and sufficiently attenuate the out-of-band blockers, which can be aliased into the desired band. As defined in Fig. 5, the lower (f_{rl}) and upper (f_{ru}) rejection frequencies are given by (18) and (19), respectively.

$$f_{rl} = Kf_s - f_l \quad (18)$$

$$f_{ru} = (K+1)f_s - f_u \quad (19)$$

The minimum out-of-band attenuation is required to bring the blocker level at the rejection frequencies to the noise floor. It is given by (14).

The IF filter is designed to place the first aliased signal back into the [0 $f_s/2$] region, attenuate all other aliased bands, due to the first subsampling, and avoid image aliasing, due to resampling. The first aliased band to be attenuated is located at $f_s - max(f_{IFn} + B_{chn}/2)$. The first images to be attenuated before IF sampling are located at $max(B_{chn}/2)$ and $min(2f_{IFn} - B_{chn}/2)$. The IF filter specifications are illustrated graphically in Fig. 6. Since image signals are located out of the desired IF band, the required attenuations for each radio standard signal can be achieved by the first and second RF filters.

IV. Design Application to GSM/UMTS/802.11g RF Subsampling Receiver

By considering the proposed RF subsampling radio receiver structure and design methodology presented in previous sections, the practical design of a multistandard GSM, UMTS and IEEE-802.11g radio receiver was carried out to validate the authors' contributions. This receiver was designed to be able to receive any one of the three standards bands: *35 MHz* centered at *942.5 MHz* for GSM, *60 MHz* centered at *2140 MHz* for UMTS or *83.5 MHz* centered at *2441.75 MHz* for IEEE-802.11g [1-3]. The design steps that are detailed in this section concern the subsampling frequency plan computation, T&H circuit design and analog filter design. System level tests and performance analysis were conducted through realistic RF-DSP co-simulation using Agilent ADS software. The proposed multistandard receiver was validated using concurrent GSM, UMTS and IEEE-802.11g signals. Receiver sensitivity analysis was also carried out.

A. Frequency plan synthesis

For each radio standard, the application of design formulations (1), (2) and (3) gave several subsampling frequencies allowing for down-conversion, without aliasing of RF signals for one of the three radio standards. For these acceptable subsampling frequencies and by applying constraints (5) and (8), optimized values were deduced: f_{sopt} (MHz) = {*569.9, 761.8*}. We considered the higher value of f_{sopt} = *761.8 MHz*, since it allows for T&H thermal noise attenuation of *1.25 dB* and aperture jitter SNR improvement of *2.5 dB*. Fig. 7 shows the derivation of IF frequencies as functions of sampling frequency using (1). Table 1 gives the resulting optimized IF frequencies for each standard after the subsampling operation. The second subsampling frequency should be equal to the desired channel center frequency at IF band. A tunable sampling clock in the IF band *(117.8 MHz - 198 MHz)* with a *0.2 MHz* tuning step is required to generate f'_{sn}.

B. Track-and-hold circuit design

We assumed a receiver RF front-end gain, G, of *25 dB* for GSM, UMTS and IEEE-802.11g standards. In order to neglect T&H thermal noise (11) versus receiver noise floor at the T&H input (12), the sampling capacitance, C_H, had to be greater than *0.2 pF*, *0.3 pF* and *0.18 pF* for GSM, UMTS

Authorized licensed use limited to: Suzanne Habib. Downloaded on February 20,2025 at 15:04:44 UTC from IEEE Xplore. Restrictions apply.

Exhibit 1020
Nokia of America Corporation, et al. v. Smart RF Inc.
Page 000005

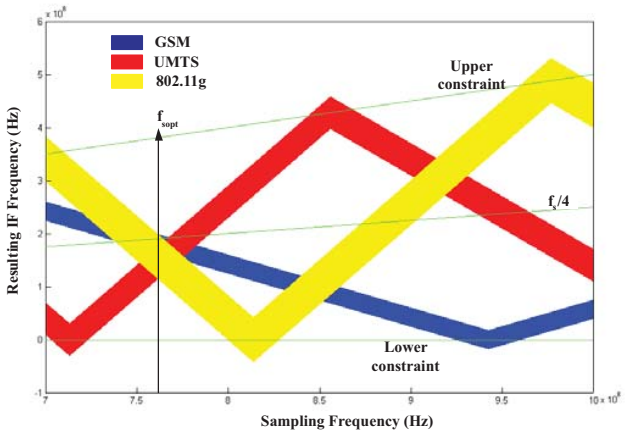

Fig. 7. Resulting IF frequencies.

TABLE I
RESULTING IF FREQUENCIES AFTER SUBSAMPLING, $f_s = 761.8MHz$.

Parameters	GSM	UMTS	802.11g
IF band (MHz)	163.2-198.2	115.4-175.4	114.6-198.1
Centered IF (MHz)	185.7	145.4	156.35
Signal type	Original	Mirrored	Original

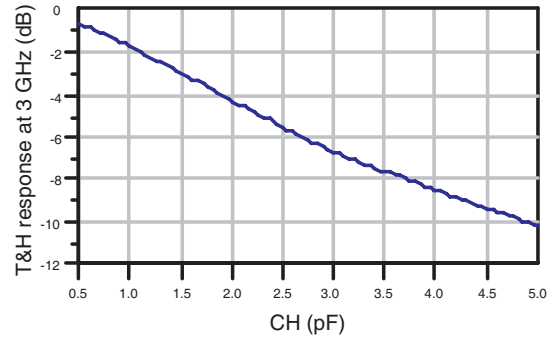

Fig. 8. T&H analog bandwidth as a function of C_H.

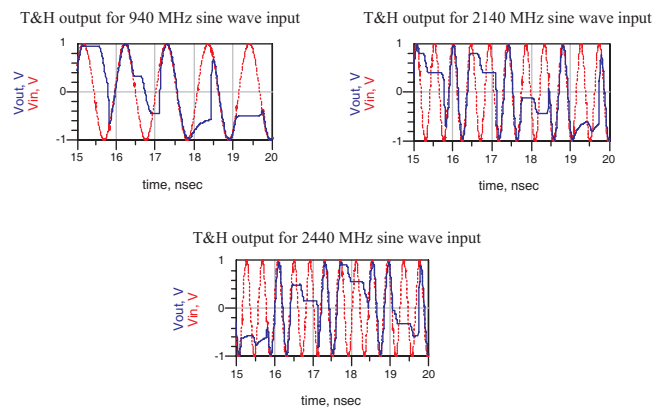

Fig. 9. T&H temporal responses.

and IEEE-802.11g standards, respectively. If G is reduced by *3 dB*, C_H has to be greater than *0.4 pF*, *0.6 pF* and *0.36 pF*. Furthermore, the T&H circuit has to be fast enough to process GSM, UMTS and IEEE-802.11g RF signals, so the T&H analog input bandwidth had to be greater than *2.45 GHz*. By considering an NMOS switch from $0.35\mu m$ CMOS library, simulation results show that C_H had to be lower than *1.5 pF* to insure an input bandwidth higher than *3 GHz*. This is illustrated by Fig. 8.

For C_H *=1 pF*, the temporal response of the T&H circuit (Fig. 4) implemented with dummy switch compensation technique has been simulated for *940 MHz*, *2140 MHz* and *2440 MHz* sine wave excitations (Fig. 9). This led to the selection of C_H = *1 pF* that allows for the T&H speed-accuracy-thermal noise trade-off. The minimum RF front end gain G that allows neglecting T&H thermal noise versus receiver noise floor at the T&H input is *20 dB*. So a gain G of *25 dB* is a reasonable choice.

By using (13), the maximum allowed aperture jitter was limited to *0.41 ps* for GSM, *1.9 ps* for UMTS and *0.27 ps* for IEEE-802.11g. Using expression (16), this can be transformed to a sampling clock phase noise of *-140 dBc/Hz*, *-127 dBc/Hz* and *-144 dBc/Hz* evaluated at the maximum blocker level for GSM, UMTS and 802.11g, respectively. The maximum input signal to the first T&H circuit is equal to the maximum receiver input signal, P_{max}, amplified by G. This gave a maximum T&H input signal of *10 dBm* corresponding to *0.7 V rms* or *2 V peak-to-peak* voltage.

Table 2 gives the first T&H circuit specifications for the GSM, UMTS and IEEE-802.11g standards. The same analysis was conducted for the second T&H circuit with $f_c = f_{IF} = f_s$ and B_{ana}*=210 MHz*. Table 3 gives the second T&H circuit specifications for the GSM, UMTS and IEEE-802.11g standards.

C. Filter design

The first RF band-pass filter response was selected with a band-pass width equal to the reception band and maximum band-pass insertion loss of *3 dB*. By considering defined filter specifications, ADS-based computer-aided design (CAD) allows for the choice of Butterworth band-pass filters that have 5th, 3rd and 3rd orders for the GSM, UMTS and IEEE-802.11g standards, respectively, to respect the specified RF filters masks [12].

Table 4 gives the computed specifications for the second or anti-aliasing RF filters. By considering defined filter specifications, ADS-based CAD allows for the choice of 2nd-order Butterworth band-pass filters for the GSM, UMTS and IEEE-802.11g to meet RF anti-aliasing filter specifications and, with the first RF filter, to offer a total minimum attenuation of *142 dB*, *92 dB* and *85 dB* for the GSM, UMTS and IEEE-802.11g maximum blockers, respectively, at rejection frequencies.

According to the RF filter specifications defined in the previous section, the required IF filter attenuations have been computed for each standard, taking into consideration the contributions of the RF filters. Table 4 gives a summary of the IF filter specifications with respect to IF channels and band. According to this result, one IF filter can be designed to meet the GSM, UMTS and IEEE-802.11g IF filter specifications simultaneously.

Authorized licensed use limited to: Suzanne Habib. Downloaded on February 20,2025 at 15:04:44 UTC from IEEE Xplore. Restrictions apply.

Exhibit 1020
Nokia of America Corporation, et al. v. Smart RF Inc.
Page 000006

TABLE II
FIRST T&H CIRCUIT SPECIFICATIONS.

Parameters	GSM	UMTS	802.11g
Analog bandwidth (GHz)	2.45		
Maximum input signal (V)	2 peak-to-peak		
Sampling capacitance (pF)	1		
Subsampling frequency (MHz)	761.8		
$f_{sn}^{'}$ (MHz)	925-960	2110-2170	2400-2483.5
DR (dB)	96	83.8	75
SNR_j (dB)	52.2	31.8	47.6
Δt (ps)	0.41	1.9	0.27
PN (dBc/Hz)	-140	-127	-144

TABLE III
SECOND T&H CIRCUIT SPECIFICATIONS.

Parameters	GSM	UMTS	802.11g
Analog bandwidth (GHz)	0.21		
Maximum input signal (V)	1.7 peak-to-peak		
Sampling capacitance (pF)	10		
Subsampling frequency (MHz)	117.8-198 (step 0.2)		
$f_{sn}^{'}$(MHz)	163.2-198.2	115.4-175.4	114.6-198.1
DR (dB)	96	83.8	75
SNR_j (dB)	58.3	39	54.5
Δt (ps)	1.05	12.2	1.9
PN (dBc/Hz)	-138	-117	-133

By fixing the maximum band-pass insertion loss to *1.5 dB*, ADS-based CAD shows that IF filter specifications were respected with a 9th-order Butterworth band-pass filter, a 5th-order Chebyshev band-pass filter, and a 5th-order Elliptic band-pass filter. After comparing the three filter types, the Chebyshev-based filter was chosen, since it gave the minimum order with an acceptable linear phase response. Fig. 10 shows the proposed IF Chebyshev filter frequency response with the established GSM/UMTS/IEEE-802.11g specified masks, as shown in Table 4.

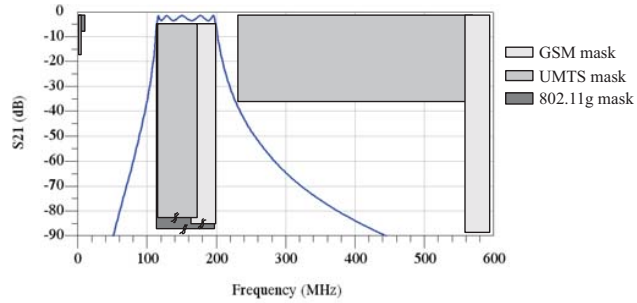

Fig. 10. IF Chebyshev filter frequency response with the specified mask.

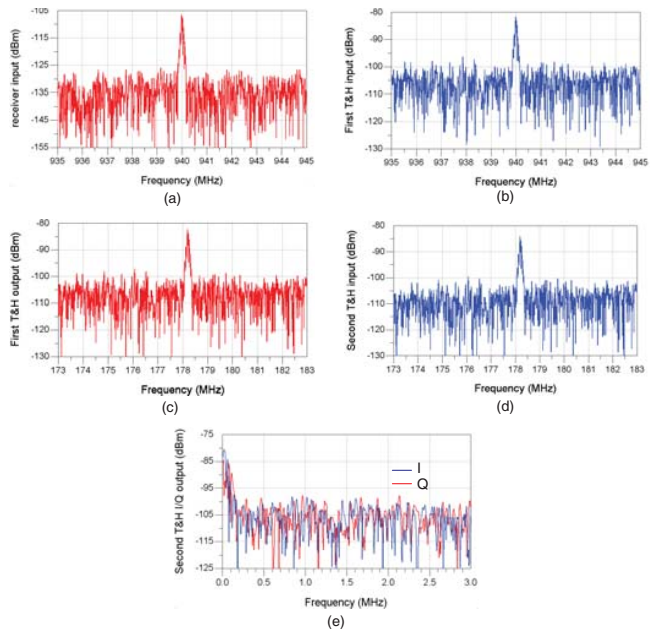

Fig. 11. GSM signal spectrum through multistandard RF subsampling receiver blocks.

D. Simulation results

The ADS model was defined to simulate proposed RF subsampling receiver performances. The ADS receiver model was built by including a first RF filter *(IL = 3 dB)*, an LNA *(Gain = 31 dB, Noise figure = 2 dB)*, an anti-aliasing RF filter *(IL = 3 dB)*, a first-order T&H circuit, an IF filter *(IL = 1.5 dB)* and a second complex subsampling stage. To test this receiver with multistandard radio signals, a modulated RF signal block was constructed for GSM/UMTS/IEEE-802.11g, based on the standards' specifications [1, 3]. RF and IF filter parameters and subsampling frequency values were set according to design results given in previous sections. The T&H circuit was implemented using sample and hold with an RF clock ADS component.

Frequency and time responses have been evaluated through the receiver using digital signal processing (DSP) simulation and a data flow controller block. Estimation of the signal spectrum was performed by computing a fast Fourier transform (FFT) on the signal that requires 2^N data points. *N = 18* was used for the FFT calculation.

Fig. 11 shows the GSM signal spectrum through the RF subsampling receiver block. As shown in Fig. 11a, we assumed that a *940 MHz* GMSK (Gaussian minimum shift keying) modulated signal with *200 kHz* bandwidth, *-99 dBm* power level and *-174 dBm/Hz* noise power spectral density is received at the antenna, based on the GSM standard [1]. Through the receiver RF front-end, the GSM channel was filtered and amplified. The total RF front-end gain was around *25 dB*. Fig. 11b and 11c show the GSM signal before and after subsampling by f_s = *761.8 MHz*. We notice that the GSM down-converted channel after the first subsampling was centered at *178.2 MHz* without SNR degradation. After the IF filter, the aliased signals were well attenuated. Fig. 11e illustrates the baseband I (inphase) and Q (quadrature) GSM components after the second subsampling stage by $f_s^{'}$ =*178.2 MHz*. This result highlights RF frequency down-conversion to baseband signals through the sampling-based down-conversion stage. The SNR degradation through RF subsampling receiver was about *6.4 dB*, which is compliant with the GSM standard for the receiver noise figure *(10 dB)*.

The same analysis was done for a *2140 MHz* QPSK

Authorized licensed use limited to: Suzanne Habib. Downloaded on February 20,2025 at 15:04:44 UTC from IEEE Xplore. Restrictions apply.

Exhibit 1020
Nokia of America Corporation, et al. v. Smart RF Inc.
Page 000007

TABLE IV
RF AND IF FILTER SPECIFICATIONS.

Parameters	GSM	UMTS	802.11g
RF filter specifications			
Cut-off frequencies (MHz)	925-960	2110-2170	2400-2483.5
Rejection frequencies (MHz)	591, 1314	1680, 2378	2148, 2822.5
A_{tt} (dB)	108	80.8	77
IF filter specifications			
Cut-off frequencies (MHz)	163.3-198.1	115.88-175.92	115.6-197.6
Rejection frequencies (MHz)	0.1, 326.7	1.92, 233.68	11, 242.2
Aliased frequency attenuation	85dB@563.6 MHz	51.8DB@586.4 MHz	60dB@563.7 MHz
Minimum image frequency attenuation without RF filtering (dB)	108	80.8	77
Minimum image frequency attenuation with RF filtering (dB)	0dB@0.1MHz 0dB@326.7MHz	1dB@1.92MHz 23dB@233.68MHz	10dB@11MHz 39dB@242.2MHz

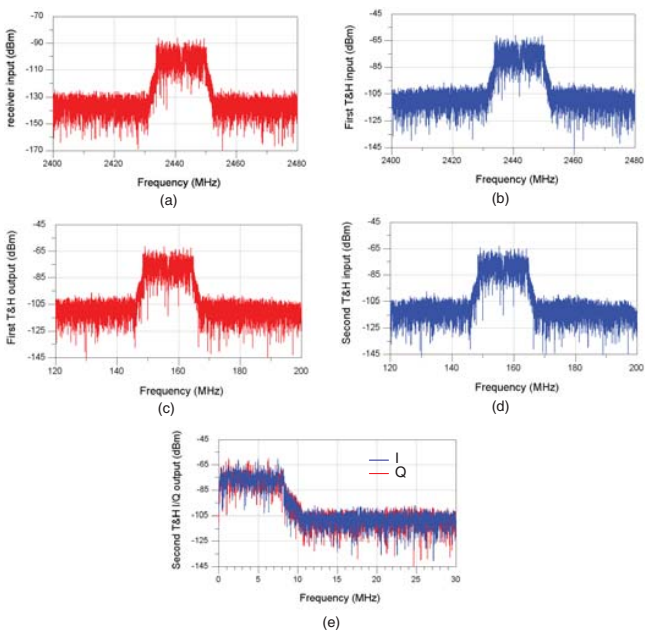

Fig. 12. ERP-OFDM signal spectrum through multistandard RF subsampling receiver blocks (54 Mpbs).

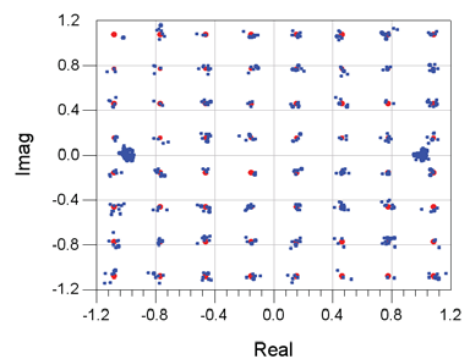

Fig. 13. WLAN signal constellation.

(quadrature phase-shift keying) modulated signal with *3.84 MHz* bandwidth and *-90 dBm* power level, based on the UMTS standard [2], and for a *2442 MHz* 64-QAM modulated signal with *22 MHz* bandwidth and *-65 dBm* power level, based on the ERP-OFDM (extended rate physical orthogonal frequency-division multiplexing) 802.11g standard with *54 Mbps* of data rate [3]. The input noise power spectral density was *-174 dBm/Hz*. Fig. 12 shows the 802.11g signal spectrums through the RF subsampling receiver block. The overall SNR degradations were about *7.5 dB* for UMTS and *7.2 dB* for 802.11g, which are less than the allowed receiver noise figures (*9.3 dB* for UMTS and *10.5 dB* for 802.11g). These results highlight the multistandard RF frequency down-conversion to IF then to baseband through the sampling-based down-conversion stage with an appropriate SNR degradation; and, they validate the multistandard receiver sensitivity tests. Simulations of the 802.11g constellation diagram at the RF subsampling receiver output for a modulation scheme of 64 QAM with a maximum data rate of *54 Mbps* is shown in Fig. 13 for 500 data points. The resulting error vector magnitude (EVM) was *4.8%* , which is less than the 802.11g tolerated EVM of *5.6%*. In the same way, we simulated the RF subsampling receiver 802.11g SNR and EVM without the second RF filter. The signal to noise ratio degradation was around *7 dB* and led to an increase in the receiver EVM of *8.5%*. Therefore, without an anti-aliasing RF filter, the wideband noise at the LNA output will be aliased due to subsampling. The second RF filter also contributes to out-of-band image blocker attenuation. Simulations of the RF subsampling receiver 802.11g SNR and EVM without an IF filter were carried out; and, the signal to noise ratio degradation was around *15 dB* and led to an increase in the receiver EVM of *10%*. Therefore, without an anti-aliasing IF filter after the second sampling stage, the aliased channels after the first subsampling and image channels would be folded into the baseband and lead to high SNR degradation.

V. CONCLUSION

A new subsampling-based down-conversion topology is proposed in this paper for multistandard radio receiver design. To overcome variable frequency sampling effects in the multistandard context, the proposed receiver topology uses two sampling stages. The first subsampling frequency is chosen to properly down-convert multistandard RF bands to a fixed IF band, which relaxes the IF filter design. Relaxed constraints are obtained for the low noise amplifier by adding a second RF filter after the first sampling stage. A second T&H circuit with tunable IF clock frequencies in the IF band is designed

Authorized licensed use limited to: Suzanne Habib. Downloaded on February 20,2025 at 15:04:44 UTC from IEEE Xplore. Restrictions apply.

Exhibit 1020
Nokia of America Corporation, et al. v. Smart RF Inc.
Page 000008

to perform desired channel quadrature down-conversion to baseband. A generic analytical design methodology for the proposed receiver topology is provided in this paper.

By considering GSM, UMTS and IEEE-802.11g multistandard specifications for the RF subsampling radio receiver design, a first subsampling frequency clock of *761.8 MHz* is chosen to down-convert different RF bands to the same IF band (*114.6 MHz - 198.2 MHz*). For the designed RF subsampling receiver, system level ADS-based simulation shows total noise figures of *6.4 dB*, *7.5 dB* and *7.2 dB* for the GSM, UMTS and IEEE-802.11g standards, respectively. Simulation results regarding the error vector magnitude values prove the RF and IF filters' design efficiency. The overall results of this practical design example confirm the validation of the proposed receiver topology and design methodology, which can be applied in the context of multistandard radio design.

Physical implementations of the T&H circuit and the IF filter switched-capacitor circuit [19] were considered in designing and assessing the multistandard RF subsampling receiver performance.

ACKNOWLEDGMENT

The authors would like to thanks Dr. M. Helaoui, Mrs. A. Bassam and Mr. R. Darraji for their inputs and suggestions.

REFERENCES

[1] ETSI, Digital cellular telecommunications system (phase 2) (GSM); radio transmission and reception (GSM 05.05), Version 5.0.0, Apr. 1996.
[2] ETSI, UE. Radio transmission and reception (FDD), (3GPP TS 25.101), Version 5.2.0 Release 5, Apr. 2002.
[3] IEEE Std, Part 11: Wireless LAN Medium Access Control (MAC) and Physical Layer (PHY) Specifications, Amendment 4: Further Higher Data Rate Extension in the 2.4 GHz Band, 802.11g, 2003.
[4] Bluetooth Specification, Part A, Radio Specification, Version 1.0 A, July 1999.
[5] B. Razavi, *RF Microelectronics*. Prentice Hall, 1998.
[6] K. Muhammad, R. B. Staszewski, and D. Leipold, "Digital RF processing: toward low-cost reconfigurable radios," *IEEE Commun. Mag.*, pp. 105-113, Aug. 2005.
[7] D. Jakonis, K. Folkesson, J. Dabrowski, P. Eriksson, and C. Svensson, "A 2.4-GHz RF sampling receiver front-end in 0.18um CMOS," *IEEE J. Solid-State Circuits*, vol. 40, pp. 1265-1277, June 2005.
[8] K. Muhammad, D. Leipold, B. Staszewski, Y. C. Ho, C. M. Hung, K. Maggio, C. Fernando, T. Jung, J. Wallberg, J. S. Koh, S. John, I. Deng, O. Moreira, R. Staszewski, R. Katz, and O. Friedman, "A discrete-time Bluetooth receiver in 0.13mm digital CMOS process," in *Proc. IEEE Int. Solid-State Circuits Conf. Dig. Tech. Papers*, Feb. 2004, pp. 268-269.
[9] Agilent website, http://eesof.tm.agilent.com/products/ads_main.html
[10] R. G. Vaughan, N. L. Scott, and D. R. White, "The theory of bandpass sampling," *IEEE Trans. Signal Processing*, vol. 39, pp. 1973-1984, Sept. 1991.
[11] D. M. Akos, M. Stockmaster, J. B. T. Tsui, and J. Cashera, "Direct bandpass sampling of multiple distinct RF signals," *IEEE Trans. Commun.*, vol. 47, pp. 983-988, July 1999.
[12] R. Barrak, A. Ghazel, and F. M. Ghannouchi, "Design and optimization of RF filters for multistandard RF sub-sampling receiver," in *Proc. IEEE Int. Design and Test of Integrated Systems in Nanoscale Technology Conf.*, Sept. 2006, pp. 105-109.
[13] D. Jakonis, "Direct RF sampling receivers for wireless systems in CMOS technology," thesis dissertation, Linköping University, Sweden, 2004.
[14] D. A. Johns and K. Martin, *Analog Integrated Circuit Design*. John Wiley & Sons, 1997.
[15] C. Eichenburger and W. Guggenbuhl, "On charge injection in analog MOS switches and dummy switch compensation techniques," *IEEE Trans. Circuits and Systems*, vol. 37, pp. 256-264, Feb. 1990.
[16] R. Gregorian and G. C. Temes, *Analog MOS Integrated Circuits for Signal Processing*. John Wiley & Sons, 1986.
[17] M. Shinagawa, Y. Akazawa, and T. Wakimoto, "Jitter analysis of high speed sampling systems," *IEEE J. Solid-State Circuits*, vol. 25, pp. 220-224, Feb. 1990.
[18] P. Eriksson and H. Tenhunen, "Phase noise in sampling and its importance to wideband multicarrier base station receivers," in *Proc. IEEE Int. Conf. Acoustics, Speech, and Signal Processing*, vol. 5, Mar. 1999, pp. 2737-2740.
[19] S. Andersson *et al.*, "SC filter for RF sampling and downconversion with wideband image rejection," *Kluwer-Springer Analog Integrated Circuits and Signal Processing*, vol. 49, pp. 115-122, 2006.

Rim Barrak received the B.S. degree in Circuits and Systems from the Ecole Polytechnique de Tunisie, Tunis, Tunisa, in 2000, and the M.S. degree in telecommunications from the Ecole Polytechnique de Montréal, Montreal, QC, Canada, in 2002 and the Ph.D. degree in communication and information technologies from the Ecole Supérieure des Communications -SUP'COM, Tunis, Tunisia in 2007. She is currently an assistant professor in Telecommunications and member of CIRTA'COM research laboratory at SUP'COM. Her research interests are in the areas of software radio receiver architectures, subsampling frequency downconversion technique and discrete-time processing for wireless communications.

Adel Ghazel (IEEE Senior Member) received the E.E and M.S. degrees in systems analysis and digital processing from the Ecole Nationale d'Ingénieurs de Tunis - (ENIT), Tunis, Tunisia, both in 1990, the Ph.D. degree in electrical engineering from ENIT and the Habilitation degree in communication and information technologies from Ecole Supérieure des Communications - SUP'COM, Tunisia in 1996 and 2002, respectively.

He is currently a Professor in Telecommunications, the Dean of Planning and CIRTA'COM Research Laboratory Director at SUP'COM. From 1990 to 1992, he worked for Tunisia Engineering and Industrial Construction Company as a Specialist Engineer. In 1993, he joined the Ecole Supérieure des Postes et des Télécommunications de Tunis and became in 1999 the Head of the Department of Electronics and Propagation at SUP'COM. Since 2001 he has been the Program Manager of the Reaserch & Development center partner of Analog Devices SST Division, Boston, MA. He has authored or coauthored over 120 publications. His current research interests include VLSI and DSPs circuits, algorithms and architectures for communications systems.

Fadhel M. Ghannouchi (S'84-M'88-SM'93) received the B.Eng. degree in engineering physics and the M.S. and Ph.D. degrees in electrical engineering from the Ecole Polytechnique de Montréal, Montreal, QC, Canada, in 1983, 1984, and 1987, respectively.

He is currently a iCORE professor and Senior Canada Research Chair at Electrical and Computer Engineering Department of The Schulich School of Engineering of the University of Calgary and Director of Intelligent RF Radio Laboratory (www.iradio.ucalgary.ca). He held several invited positions at several academic and research institutions in Europe, North America and Japan. He has provided consulting services to a number of microwave and wireless communications companies. His research interests are in the areas of microwave instrumentation and measurements, nonlinear modeling of microwave devices and communications systems, design of power and spectrum efficient microwave amplification systems and design of intelligent RF transceivers for wireless and satellite communications. His research activities led to over 400 publications and 10 US patents (three pending). Professor Ghannouchi is a Fellow IEEE, Fellow IET and a Distinguish Microwave Lecturer for IEEE-MTT Society.

Authorized licensed use limited to: Suzanne Habib. Downloaded on February 20,2025 at 15:04:44 UTC from IEEE Xplore. Restrictions apply.

Exhibit 1020
Nokia of America Corporation, et al. v. Smart RF Inc.
Page 000009